Stress-relaxation in bending of Inconel 718, at 773 and 823 K

F. POVOLO
Comisión Nacional de Energía Atómica, Dto. de Materiales, Av. del Libertador 8250, (1429) Buenos Aires, and Universidad de Buenos Aires, Facultad de Ciencias Exactas y Naturales, Dto. de Física. Pabellón 1, Ciudad Universitaria, (1428) Buenos Aires, Argentina

J. F. REGGIARDO
Universidad Tecnológica Nacional, Facultad Regional S. Nicolás, C.C. 118, (2900) San Nicolás, Argentina

Stress-relaxation data in Inconel 718, both at 773 and 823 K and up to times of the order of 4000 h, in specimens with different thermal treatments, are presented. No substantial differences are encountered, between 773 and 823 K, in the stress-relaxation behaviour of the age-hardened material. In the as-received and the solution-annealed specimens, on the contrary, the stress-relaxation curves indicate that the structure does not remain stable during relaxation and the internal stress decreases continuously as the applied stress decreases. The structure is stable, for all the thermal treatments, during stress relaxation at 773 K. Finally, the data are interpreted in terms of an interaction between gliding dislocations and precipitates as indicated by the large activation volumes involved and the negligible influence of thermal activation.

1. Introduction

Nickel superalloys are widely used in applications which require high creep, fatigue and corrosion resistance at elevated temperatures. The high creep strength of these materials depends on such factors as solid solution hardening of the f c c γ matrix, grain-boundary strengthening by carbides and most importantly, on the ability of precipitates of the ordered ($L1_2$) intermetallic γ' phase to impede dislocation motion [1]. The stress-relaxation behaviour of nickel superalloys is also important, both from the practical and academic points of view, but only few data are available in the literature on the stress relaxation of these alloys. Kennedy and Douglas [2] studied the creep and relaxation characteristics of Inconel 600 at temperatures between about 978 and 1172 K, initial stresses between 65 and 196 MPa and times up to 100 h. The stress-relaxation data, obtained both in the as-received material with a fine-grain size and in a coarse-grained structure obtained by re-annealing the as-received material at 1394 K for 1 h, lead to straight lines in a $\log \sigma$–$\log \dot{\varepsilon}$ representation, where σ is the applied stress and $\dot{\varepsilon}$ the plastic strain rate. This would indicate that the creep and stress-relaxation data can be described by an expression of the type (Norton's creep equation)

$$\dot{\varepsilon} = A\sigma^n \qquad (1)$$

where n and A are constants. Furthermore, values between 4.79 and 6.18 were obtained for n. Osthoff *et al.* [3] studied the creep and relaxation behaviour of Inconel-617, in the temperature region between 1023 and 1073 K. The relaxation tests were carried out on specimens that reached the primary or secondary creep region and only relaxation experiments done in the secondary creep region were presented. According to these authors, the relaxation behaviour was more satisfactorily described by using the Norton's creep equation modified by the internal stress than by using the conventional equation (Equation 1), that is, by the expression

$$\dot{\varepsilon} = A^*(\sigma - \sigma_i)^{n^*} \qquad (2)$$

where A^* and n^* are constants and σ_i is an internal stress. Furthermore, $n = 2n^*$ was found to be of the order of 6 and the internal stress varied between about 16 and 40 MPa, decreasing with increasing temperature.

The only stress-relaxation data available in the literature, on the relaxation behaviour of Inconel-718 are those reported by Huntington Alloys [4], for helicoidal springs made with age-hardened material. The data were obtained at 811 and 866 K, up to times of the order of 1000 h and initial stresses of the order of 414 MPa. These results are presented by the manufacturer only for illustration and no attempt is made to interpret them analytically.

It is the purpose of this paper to present data on the stress-relaxation behaviour, in bending and at 773 and 823 K, of Inconel-718. Three different thermomechanical treatments are given to the specimens prior to the stress-relaxation experiments and the measurements were extended up to times of the order of 4000 h at various initial stresses.

0022–2461/88 $03.00 + .12

TABLE I Chemical composition of the Inconel 718 used

Element	Composition (wt %)
C	0.05
Si	0.15
Mn	0.13
P	0.004
S	0.004
Cr	18.8
Ni	51.8
Co	0.037
Mo	3.1
Ti	0.9
Al	0.44
Fe	19.19
Cu	0.05
Ta	0.05
Nb	4.95

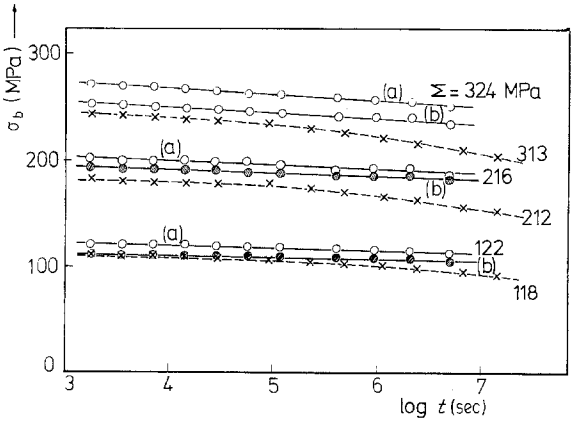

Figure 1 Measured stress change at the surface as a function of time for Type A specimens. (——) Data obtained at 773 K, (– – –) data obtained at 823 K. The corresponding initial stresses are given on each curve.

2. Experimental procedure

2.1. Specimen preparation

The original material was supplied by Inco-Huntington (West Virginia, USA) in the form of sheets 0.52 mm thick. The composition of the alloy, as supplied by the manufacturer, is given in Table I.

The specimens were prepared with the axis parallel to the rolling direction and, in addition to the as-received condition, two different thermal treatments were used, prior to the stress-relaxation measurements. In fact, some of the specimens (15 mm wide and 100 mm long) were carefully cleaned and sealed into fused silica tubes with argon atmosphere. These tubes were heated 1 h at 1255 K and dropped into oil for a quenching treatment. Part of these specimens were heat-treated into a fused silica tube connected to a high-vacuum equipment, at 991 K for 8 h and cooled down, in 2 h, to 893 K where they were maintained in vacuum for 16 h and subsequently cooled by removing from the furnace ("air cooling"). These different thermal treatments are named A, B and C, respectively, as indicated in Table II.

2.2. Stress-relaxation measurements

The specimens, originally flat, were bent elastically into stainless steel holders with radii which gave maximum outer fibre stresses between approximately 120 and 320 MPa. The holders are similar to those described by Fraser *et al.* [5]. The holders with the specimens were inserted into a furnace either at 773 or 823 K and extracted periodically for curvature measurements. The temperature was controlled with thermocouples attached to the holders near the specimens and the fluctuations were of the order of ± 1 K. The radii of curvature, R_i, after releasing the specimens from the holders were determined by measuring the coordinates of different points with respect to a reference plane, in the arc of circumference determined by the curved beam and feeding the data to a computer program which calculated the average radius by a least square fitting. Duplicate specimens were used in order to observe the dispersion between equivalent specimens in the results. The stresses at the surface of the beam, σ, before unloading were determined by the relationship [6, 7]

$$\sigma = \tfrac{2}{3}\sigma_b + \frac{\Sigma}{3}\frac{d\sigma_b}{d\Sigma} \quad (3)$$

where $\Sigma = Eh/2R$ is the initial stress at the surface of the bent specimen and

$$\sigma_b = \frac{Eh}{2}\left(\frac{1}{R_i} - \frac{1}{R}\right) \quad (4)$$

the measured stress change in the same position, after releasing the specimen from the holder. h is the thickness of the specimen, R is the radius of curvature of the holder and E is Young's modulus (182 GPa at 773 K and 170 GPa at 823 K [4]).

TABLE II Thermal treatments given to the specimens prior to the stress-relaxation tests

Thermal treatment	Name
As-received	A
A + 1 h at 1255 K in argon and oil-quenched	B
A + B + 8 h at 991 K, cooled in 2 h to 893 K and 16 h at this temperature, all in vacuum, and "air-cooled"	C

3. Results

Fig. 1 shows the measured stress change at the surface of Type A specimens for various initial stresses. The full curves represent data obtained at 773 K and the broken curves measurements performed at 823 K. Similar data obtained in Type B and Type C specimens are shown in Figs 2 and 3, respectively.

It is seen that in some cases, for example the full curves for $\Sigma = 324$ MPa at the top of Fig. 1, equivalent specimens can give slightly different results (Curves a and b). This is because even if both specimens had the same termomechanical treatment, there might be a slight difference in the initial state of the material. When only one curve is shown, for a given Σ, the data correspond to the average value for two equivalent specimens. The stresses, σ, at the surface of the specimen before unloading, which correspond to the values that would be obtained, in the same material, under initial uniaxial stresses given by Σ, can

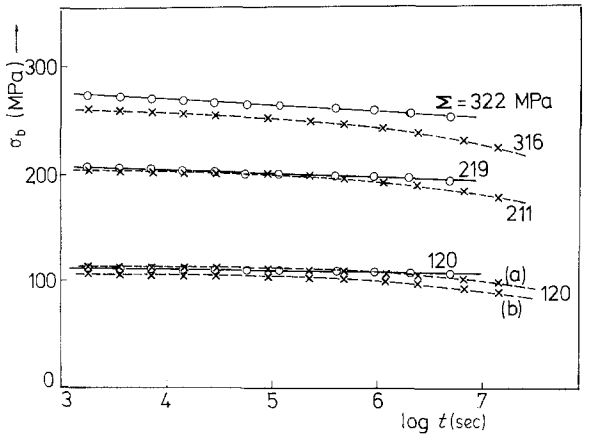

Figure 2 Measured stress change at the surface as a function of time for Type B specimens. (——) Data obtained at 773 K, (– – –) data obtained at 823 K. The corresponding initial stresses are given on each curve.

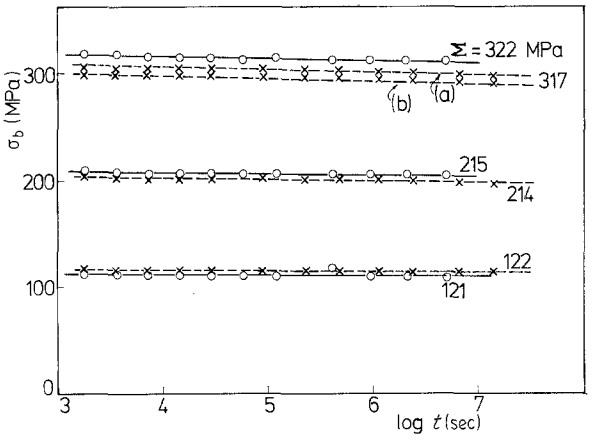

Figure 3 Measured stress change at the surface as a function of time for Type C specimens. (——) Data obtained at 773 K, (– – –) data obtained at 823 K. The corresponding initial stresses are given on each curve.

be calculated by using Equation 3. In fact, as shown by Figs 1 to 3, all the measurements performed at 773 K lead to a linear behaviour of σ_b with log t. A similar situation was found for the data obtained at 823 K in Type C specimens. This means that in the region of stresses and times considered, the curves are described by the expression

$$\sigma_b = A(\Sigma) - B(\Sigma) \log t \quad (5)$$

On taking into account Equation 3, it is easy to show that σ is given in this case by

$$\sigma = A^*(\Sigma) - B^*(\Sigma) \log t \quad (6)$$

where

$$A^*(\Sigma) = \tfrac{2}{3} A(\Sigma) + \frac{\Sigma}{3} \frac{dA(\Sigma)}{d\Sigma} \quad (7)$$

and

$$B^*(\Sigma) = \tfrac{2}{3} B(\Sigma) + \frac{\Sigma}{3} \frac{dB(\Sigma)}{d\Sigma} \quad (8)$$

A plot of A and B as a function of Σ, for each type of specimen, shows that both parameters change linearly with Σ and, consequently, both $dA/d\Sigma$ and $dB/d\Sigma$ are constants. Table III gives the parameters obtained for the different curves, at both temperatures for Type C specimens and at 773 K for Type A and Type B specimens. Furthermore, according to Equations 6, 7 and 8 and the values given in Table III it is seen that σ has the same time-dependence as σ_b with quite similar values.

As shown by Figs 1 to 3, the data obtained in Type A and Type B specimens at 823 K lead to curves in the σ_b against log t representation. A plot of log σ_b against log Σ at different times, however, leads to straight lines with the same slope for each type of specimen. This would indicate that σ_b can be expressed by

$$\sigma_b = a(t)\, \Sigma^b f(t) \quad (9)$$

where log a and b are the intercepts and the slopes, respectively, of the linear plots of log σ_b against log Σ, for different times. $f(t)$ is a general function of the time and $a(t)$ expresses the fact that the intercepts depend on the time selected. On taking into account Equations 3 and 9 it is easy to show that

$$\sigma = (\sigma_b/3)(b + 2) \quad (10)$$

TABLE III Parameters for Equations 5 and 6, for the description of the stress-relaxation behaviour of all the specimens at 773 K and Type C specimens at 823 K. All the parameters were obtained by a least-square fitting to the experimental data

Specimen	T (K)	Σ (MPa)	A (MPa)	B $\left(\frac{\text{MPa}}{\log \text{sec}}\right)$	$\frac{dA}{d\Sigma}$	$\frac{dB}{d\Sigma}$ (1/log sec)	A^* (MPa)	B^* $\left(\frac{\text{MPa}}{\log \text{sec}}\right)$
Type A	773	324(*a*)	291	5.90	0.78	0.018	278	5.87
		324(*b*)	270	5.04			263	5.30
		216(*a*)	213	3.49			198	3.62
		216(*b*)	204	3.07			192	3.34
		122(*a*)	129	2.07			117	2.11
		122(*b*)	118	1.64			110	1.82
Type B	773	322	292	5.62	0.88	0.020	289	5.92
		219	218	3.56			209	3.85
		122	117	1.58			114	1.87
Type C	773	322	324	2.03	1.04	0.0065	328	2.05
		215	212	0.97			216	1.11
		121	114	0.74			118	0.76
	823	317(*a*)	313	1.93	0.98	0.0078	312	2.11
		317(*b*)	307	2.30			309	2.36
		214	208	1.34			209	1.45
		122	118	0.59			119	0.71

TABLE IV Parameter b for Equation 10, for the curves obtained at 823 K in Type A and Type B specimens

Specimen	b
Type A	0.93
Type B	0.81

This equation shows that σ has the same time dependence as σ_b. The parameter b, for Type A and Type B specimens, for the curves measured at 823 K, are given in Table IV.

The $\log\sigma$–$\log\dot{\varepsilon}$ stress-relaxation curves are obtained by taking the derivatives of the σ against t curves, because $\dot{\varepsilon} = -\dot{\sigma}/E$; the dot indicates a derivative with respect to time. In the case where σ is described by Equation 6 it is easy to show that

$$\dot{\varepsilon} = B^*(\Sigma) \log e/t\, E \tag{11}$$

and when σ is described by Equation 10

$$\dot{\varepsilon} = -\frac{\dot{\sigma}_b}{3}\frac{(b+2)}{E} \tag{12}$$

The different $\log\sigma$–$\log\dot{\varepsilon}$ stress-relaxation curves are shown in Figs 4 to 6. It is seen that $\log\sigma$ changes linearly with $\log\dot{\varepsilon}$ at 773 K. A similar situation is found for Type C specimens at 823 K. Then, these stress-relaxation curves are described by

$$\log\sigma = \log c + d\log\dot{\varepsilon} \tag{13}$$

The parameters c and d for the different curves, obtained by a least square fitting to the data, are given in Table V. The $\log\sigma$–$\log\dot{\varepsilon}$ representation for the curves measured in Type A and Type B specimens at 823 K leads to concave downward curves, as shown by Figs 4 and 5. These data can be very well described by Hart's equation for high homologous temperatures [8], that is, by the expression

$$\ln(\sigma^*/\sigma) = (\dot{\varepsilon}^*/\dot{\varepsilon})^\lambda \tag{14}$$

where σ^* is the hardness, λ is a temperature-independent parameter and $\dot{\varepsilon}$ depends on temperature, heat treatment and deformation. A different fitting procedure from that proposed elsewhere [9, 10] was used to describe the experimental curves by Equation 14. In fact, as shown by Figs 4 and 5, the curvature is very small and the use of the derivative $d\log\sigma/d\log\dot{\varepsilon}$ leads to large errors. In these conditions it was more convenient to represent Equation 14 as

$$\ln\sigma = \ln\sigma^* - (\dot{\varepsilon}^*)^\lambda\,(1/\dot{\varepsilon})^\lambda \tag{15}$$

showing that a plot of $\ln\sigma$ against $(1/\dot{\varepsilon})^\lambda$ should lead to a straight line with slope $(\dot{\varepsilon}^*)^\lambda$ and intercept $\ln\sigma^*$. By using a least square fitting procedure with a pocket computer, λ was changed until $\ln\sigma$ against $(1/\dot{\varepsilon})^\lambda$ gave the best correlation coefficient to a straight line. Once λ is known it is easy to determine σ^* and $\dot{\varepsilon}^*$. It was found, through this procedure, that the experimental $\log\sigma$–$\log\dot{\varepsilon}$ curves could be described with an accuracy better than 1% with $\lambda = 0.28$ and the parameters σ^* and $\dot{\varepsilon}^*$ given in Table VI.

TABLE V Parameters for Equation 13, for the $\log\sigma$–$\log\dot{\varepsilon}$ stress-relaxation curves at 773 K and for Type C specimens at 823 K

Specimen	T (K)	Σ (MPa)	c (MPa sec^d)	d
Type A	773	324(a)	313	1.023×10^{-2}
		324(b)	295	9.69×10^{-3}
		216(a)	220	8.75×10^{-3}
		216(b)	212	8.26×10^{-3}
		122(a)	131	8.75×10^{-3}
		122(b)	121	7.82×10^{-3}
Type B	773	322	319	9.88×10^{-3}
		219	233	8.79×10^{-3}
		122	125	7.80×10^{-3}
Type C	773	322	339	2.77×10^{-3}
		215	222	2.30×10^{-3}
		121	123	2.88×10^{-3}
	823	317(a)	324	3.04×10^{-3}
		317(b)	322	3.44×10^{-3}
		214	217	3.12×10^{-3}
		122	123	2.68×10^{-3}

(a) and (b) are used in Equations (9), (10)
(c) and (d) are used in Equation (13)

TABLE VI Parameters used to fit the $\log\sigma$–$\log\dot{\varepsilon}$ stress relaxation curves for Type A and Type B specimens at 823 K, to Equation 14 with $\lambda = 0.28$

Specimen	Σ (MPa)	σ^*(MPa)	$\dot{\varepsilon}^*$(sec^{-1})
Type A	313	234	1.30×10^{-14}
	212	176	1.02×10^{-14}
	118	106	5.66×10^{-15}
Type B	316	261	7.59×10^{-15}
	211	211	9.26×10^{-15}
	120(a)	120	1.08×10^{-14}
	120(b)	113	2.57×10^{-14}

4. Discussion

The very well known equation that describes the plastic strain rate in terms of thermally activated dislocation motion is [11]

$$\dot{\varepsilon} = \dot{\varepsilon}_1 \exp\left[-\Delta G(\bar{\sigma})/kT\right] \tag{16}$$

where $\dot{\varepsilon}_1$ is a general pre-exponential factor, T is the absolute temperature, k is the Boltzmann constant, ΔG is the change in the free enthalpy and $\bar{\sigma} = \sigma - \sigma_i$ is the effective stress. If ΔG is expressed as

$$\Delta G(\bar{\sigma}) = \Delta G_0 - \Delta G^m(\bar{\sigma}) \tag{17}$$

Equation 16 can be written as

$$\dot{\varepsilon} = \dot{\varepsilon}_0 \exp\left[\Delta G^m(\bar{\sigma})/kT\right] \tag{18}$$

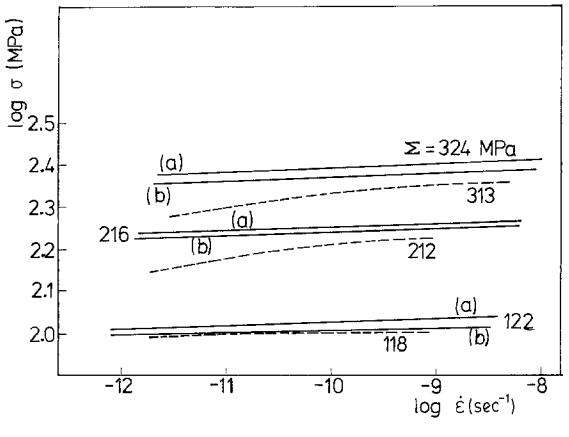

Figure 4 Stress against strain-rate relaxation curves for the Type A specimens of Fig. 1. (——) 773 K, (– – –) 823 K.

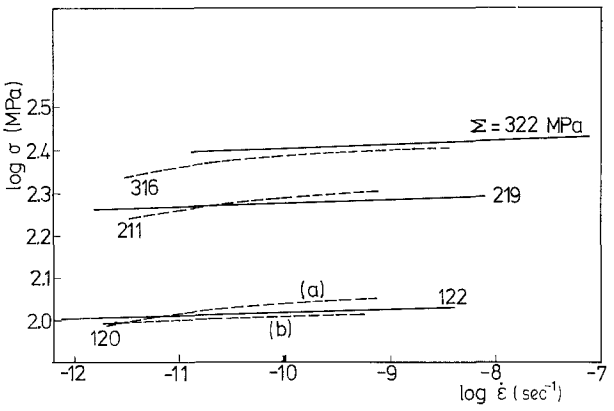

Figure 5 Stress against strain-rate relaxation curves for the Type B specimens of Fig. 2. (——) 773 K, (– – –) 823 K.

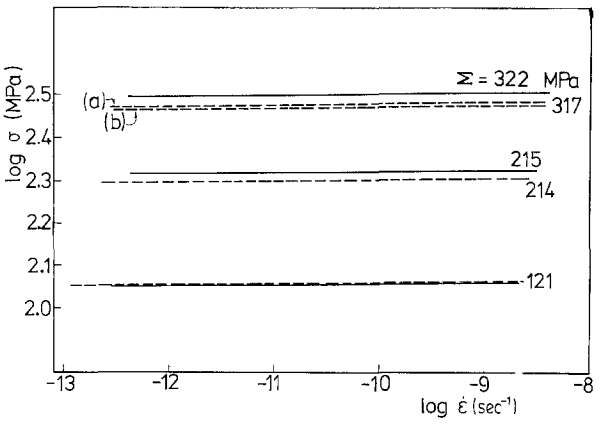

Figure 6 Stress against strain-rate relaxation curves for the Type C specimens of Fig. 3. (——) 773 K, (– – –) 823 K.

where

$$\dot{\varepsilon}_0 = \dot{\varepsilon}_1 \exp\left[-\Delta G_0/kT\right] \tag{19}$$

and $\Delta G^m(\bar{\sigma})$ gives the contribution to the change in the free enthalpy due to the applied stress.

As shown by Povolo and Tinivella [9] the Johnston–Gilman equation,

$$\dot{\varepsilon} = \phi\varrho \boldsymbol{b} v_0 (\bar{\sigma}/\sigma_0)^{m^*} = \dot{\varepsilon}_{J\text{–}G}(\bar{\sigma}/\sigma_0)^{m^*} \tag{20}$$

with

$$\dot{\varepsilon}_{J\text{–}G} = \phi\varrho \boldsymbol{b} v_0 \tag{21}$$

where ϕ is an orientation factor, ϱ is the mobile dislocation density, $\boldsymbol{b}$ is the Burgers vector and v_0, σ_0 and m^* are material constants, can be written in the form of Equation 18 if

$$\Delta G^m(\bar{\sigma})|_{J\text{–}G} = m^* kT \ln(\bar{\sigma}/\sigma_0) \tag{22}$$

and

$$\dot{\varepsilon}_0 = \phi\varrho \boldsymbol{b} v_0 = \dot{\varepsilon}_{J\text{–}G} \tag{23}$$

Furthermore, as also shown by Povolo and Tinivella [9], Hart's equation for high homologous temperature, that is, Equation 14, can be written in the form of Equation 18 if

$$\Delta G^m(\bar{\sigma})|_H = -(kT/\lambda) \ln[\ln(\sigma^*/\sigma)] \tag{24}$$

and

$$\dot{\varepsilon}_0 = \dot{\varepsilon}^* \tag{25}$$

Equation 20 reduces to Equation 14 if the internal stress changes according to the law

$$\sigma_i = \sigma - \sigma_0[\ln(\sigma^*/\sigma)]^{-1/\lambda m^*} \tag{26}$$

for $\sigma < \sigma^*$.

The activation volume, defined by

$$V^* = -\partial \Delta G^m(\bar{\sigma})/\partial\bar{\sigma}|_T \tag{27}$$

in the case of the Johnston–Gilman equation reduces to

$$V^* = kTm^*/\bar{\sigma} \tag{28}$$

and, in the case of Hart's equation to

$$V^* = \frac{m^* kT}{\sigma_0} \ln(\sigma^*/\sigma)^{1/\lambda m^*} \tag{29}$$

The interpretation of the experimental $\log\sigma$–$\log\dot{\varepsilon}$ curves will be based on the following argument: it will be assumed that the stress-relaxation curves are described actually by Equation 18 with unknown $\Delta G^m(\bar{\sigma})$ and $\dot{\varepsilon}_0$. When the representation of $\log\sigma$ against $\log\dot{\varepsilon}$ is linear, Equation 18 reduces to Equation 20 and the data are described by the Johnston–Gilman equation. If the curves show a downward curvature, Equation 18 reduces to Equation 14 and the data are described by Hart's equation for high homologous temperatures, or, which is equivalent, by the Johnston–Gilman equation with an internal stress that varies with the applied stress according to Equation 26. In fact, if the applied stress is much higher than the internal stress, Equation 20 reduces to

$$\dot{\varepsilon} = \dot{\varepsilon}_{J\text{–}G}(\sigma/\sigma_0)^{m^*} \tag{30}$$

which can be written as

$$\log\sigma = \log(\sigma_0/\dot{\varepsilon}_{J\text{–}G}^{1/m^*}) + \frac{1}{m^*}\log\dot{\varepsilon} \tag{31}$$

Then, a plot of $\log\sigma$ against $\log\dot{\varepsilon}$ leads to a straight line with slope $1/m^*$ and intercept $(\sigma_0^{m^*}/\dot{\varepsilon}_{J\text{–}G})^{1/m^*}$. This is actually the case for the data obtained for all the specimens at 773 K and for Type C specimens at 823 K, because it has been shown that they can be described by Equation 13, with the parameters given in Table V. Furthermore, on comparing Equation 31 with Equation 13 it is easy to show that

$$d = 1/m^* \quad \text{and} \quad c = (\sigma_0^{m^*}/\dot{\varepsilon}_{J\text{–}G})^{1/m^*} \tag{32}$$

According to Table V, d has similar values for Type A and Type B specimens and changes only slightly with the initial stress Σ. Then, on taking an average value leads to

$$m^* \simeq 113 \text{ for Type A and Type B specimens at 773 K} \tag{33}$$

Furthermore, d also changes slightly with Σ for Type C specimens, both at 773 and 823 K and on taking average values leads to

$$m^* \simeq 377\ (773\text{ K}) \quad \text{and} \quad m^* \simeq 326\ (823\text{ K}) \tag{34}$$

Once m^* is known, the activation volume can be calculated with Equation 28, with $\bar{\sigma} = \sigma$ as $\sigma \gg \sigma_i$. The activation volumes calculated with the values for

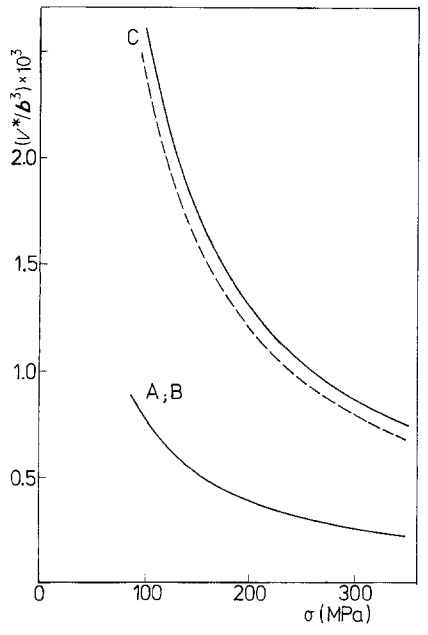

Figure 7 Relative activation volumes against stress, for different thermal treatments. (——) 773 K, (– – –) 823 K.

m^* given by Equations 33 and 34 are shown in Fig. 7 as (V^*/b^3) against σ, where $b = 2.491 \times 10^{-10}$ m, appropriate for nickel [4]. It is seen that higher activation volumes are obtained for Type C specimens, which have been age-hardened. This result is consistent with an increase of the precipitates in these specimens with respect to Type A and Type B specimens. In addition, according to Equation 28

$$m^* = \sigma V^*/kT \qquad (35)$$

showing that m^* gives the ratio between the work of external forces and the thermal energy contribution to the overcoming of the obstacles by the moving dislocations. The high m^* values obtained indicate that thermal activation is not important and the overcoming of the obstacles is mainly due to the work of external forces. The ageing treatment at 893 K changes the distribution and size of the γ' particles, increasing m^* for Type C specimens. Furthermore, no essential differences are found between 773 and 823 K in the stress-relaxation behaviour of Type C specimens. This should be expected because the precipitates are stable and thermal activation is not important.

It is important to notice at this point that similar results were obtained during measurements of the stress-relaxation behaviour, in bending and at 773 K, in an A-286 alloy which is a γ'-hardened austenitic steel [9]. In fact, high m^* values (between about 80 and 270) and activation volumes of the order of 500 b^3 were obtained for the specimens age-hardened at 993 K. Moreover, the log σ–log $\dot{\varepsilon}$ trajectories were linear indicating that the internal stress is negligible. The problem with the evaluation of the physical parameters corresponding to the stress-relaxation curves for Type A and Type B specimens, at 823 K, is that the activation volume (Equation 29) and the internal stress (Equation 26) depend on the unknown parameter σ_0. A procedure for the evaluation of this parameter was presented elsewhere [10] for the particular case in which the stress-relaxation curves showed mixed

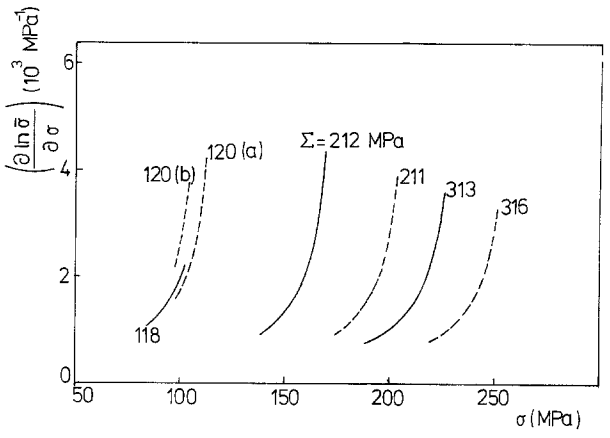

Figure 8 Rate of change of the effective stress with the applied stress against the applied stress for Type A (full curves) and Type B (broken curves) specimens, at 823 K.

curvature. This is not the case for the data obtained at 823 K, where only concave downward curves are present. Furthermore, on rearranging and differentiating Equation 26 it is easy to show that

$$(\partial \ln \bar{\sigma}/\partial\sigma)_T = 1/\lambda m^* \sigma \ln (\sigma^*/\sigma) \qquad (36)$$

which allows a calculation of the rate of change of the effective stress with the applied stress, without knowing the parameter σ_0. Equation 36 is plotted in Fig. 8 as $(\partial \ln \bar{\sigma}/\partial\sigma)_T$ against σ for the data obtained in Type A and Type B specimens at 823 K. It is seen that the effective stress and, consequently, the internal stress, changes in a complicated way with the applied stress. In addition, Equation 26 shows that the internal stress decreases continuously as the applied stress decreases, that is, as relaxation takes place. This means that the internal structure of the specimens, for treatments A and B, is not stable at 823 K, probably due to a thermal and stress-assisted evolution of the precipitates. In fact, Stevens and Flewitt [12] have examined the origin of friction stress in precipitation-hardened alloys, showing that this stress varies in a complicated way with the applied stress and three regions are observed: one at low applied stresses where the friction stress increases on increasing the applied stress; a second one, at intermediate applied stresses, where the friction stress either increases less rapidly or remains constant with increasing applied stress; a third region, at high applied stresses, where the friction stress decreases with the applied stress. Dobes and Cadek [13] reported some creep data in two γ'-hardened Ni–Al alloys, in the temperature region between 873 and 1073 K. According to these authors, in some of the alloys the effective stress increased linearly with the applied stress, at all temperatures, that is

$$\sigma - \sigma_i = \alpha\sigma + \beta \qquad (37)$$

where α and β depend on temperature. Equation 37 can be written as

$$\sigma_i = (1 - \alpha)\,\sigma - \beta \qquad (38)$$

and as $\alpha < 1$ and $\beta < 0$ it is seen that the internal stress increases linearly with the applied stress. In another alloy, the authors found that the logarithm of the effective stress increased linearly with the applied

stress, that is,

$$\ln (\sigma - \sigma_i) = \alpha'\sigma + \beta' \quad (39)$$

This equation can be written as

$$\sigma_i = \sigma - \exp(\beta') \exp(\alpha'\sigma) \quad (40)$$

and as $\alpha' > 0$, Equation 40 indicates that σ_i decreases as σ decreases.

An analysis of the stress-relaxation data is complicated further by the fact that Inconel 718 usually contains more than one precipitate [14, 15], leading to a combination of several strengthening mechanisms. Furthermore, the possible mechanisms controlling the mechanical behaviour of superalloys are still controversial [12, 13, 16–19], particularly in the temperature region used in this paper. In fact, most of the creep data are obtained at higher temperatures and, consequently, different mechanisms might be involved. As pointed out in Section 1, stress-relaxation data are very scarce.

McLean [18] has discussed recently the current models describing dislocations by-passing particles. In particular, particle shearing either by fracture of incoherent particles or by glide of dislocation pairs through coherent particles, and, bowing between particles (Orowan bowing) depend little on temperature. In addition, the threshold stresses for these mechanisms are very sensitive to the particle volume fraction, largely through its effect on the interparticle spacing, and large activation volumes should be expected. Based on the information available in the literature and without a detailed study of the evolution of the microstructure of the specimens used, it is difficult to establish, precisely, the mechanism controlling the stress-relaxation behaviour of Inconel 718, at temperatures near 773 K. It can only be stated, in general, that dislocation glide is mainly controlled by an interaction with the precipitates.

Finally, it is interesting to point out that Fox *et al.* [20] observed the formation of chromium-rich M_6C carbide in Inconel 718, creep tested at 923 K. This carbide did not form in specimens aged between 773 and 1023 K, that is, the combined action of stress and temperature is apparently needed to form M_6C. It is evident that further work is needed.

5. Conclusions

The stress-relaxation behaviour of Inconel 718, at 773 and 823 K and times of the order of 4000 h, is mainly controlled by the movement of gliding dislocations which interact with precipitates as indicated by the large activation volumes involved and the negligible influence of thermal activation. The age-hardened specimens showed much larger activation volumes, than both the as-received and the solution-annealed specimens, and no essential differences were obtained in the stress-relaxation curves measured at 773 K and at 823 K.

The stress-relaxation behaviour at 823 K, of both the as-received and the solution-annealed specimens, indicates that the structure is unstable at this temperature and changes continuously during the relaxation. In fact, the internal stress decreases in a complicated way as the applied stress decreases, probably due to a temperature- and stress-assisted evolution of the precipitates. Finally, the structure of all the specimens is stable at 773 K.

Acknowledgements

This work was supported partially by the Consejo Nacional de Investigaciones Científicas y Técnicas (CONICET), by the Comisión de Investigaciones Científicas de la Provincia de Buenos Aires and the "Programa Multinacional de Tecnología de Materiales" OAS-CNEA.

References

1. N. S. STOLOFF, in "The Superalloys", edited by C. T. Sims and W. C. Hagel, (Interscience, Now York, 1972) pp. 79–111.
2. C. R. KENNEDY and D. A. DOUGLAS, Oak Ridge National Laboratory Report ORNL-2407 (February 1960).
3. W. OSTHOFF, H. SCHUSTER, P. J. ENNIS and H. NICKEL, *Nucl. Technol.* **66** (1984) 296.
4. "Handbook of Huntington Alloys", Huntington Alloys, Inc., Huntington, West Virginia, U.S.A.
5. D. E. FRASER, P. A. ROS-ROS and A. R. CAUSEY, *J. Nucl. Mater.* **46** (1973) 281.
6. F. POVOLO and E. H. TOSCANO, *ibid.* **74** (1978) 76.
7. *Idem, ibid.* **78** (1978) 217.
8. E. W. HART, *Trans. J. Eng. Mater. Technol.* **98** (1976) 193.
9. F. POVOLO and R. TINIVELLA, *J. Mater. Sci.* **19** (1984) 1851.
10. *Idem, ibid.* **19** (1984) 2373.
11. U. F. KOCKS, A. S. ARGON and M. F. ASHBY, *Prog. Mater. Sci.* **19** (1975) 303.
12. R. A. STEVENS and P. E. J. FLEWITT, *Acta Metall.* **29** (1981) 867.
13. F. DOBES and J. CADEK, *Metall. Trans.* **3A** (1977) 1809.
14. D. J. LLOYD, in "Strength of Metals and Alloys", edited by H. J. McQueen, J.-P. Bailon, J. I. Dickson, J. J. Jonas and M. G. Akben, Vol. 3 (Pergamon, Oxford, 1985) p. 1745.
15. D. F. PAULONIS, J. M. OBLAK and D. S. DUVALL, *Trans. ASM* **62** (1969) 611.
16. A. BALDAN, *Phys. Status Solidi (a)* **83** (1984) 507.
17. C. CARRY and J. L. STRUDEL, *Acta Metall.* **25** (1977) 767.
18. M. McLEAN, *ibid.* **33** (1985) 33.
19. J. M. OBLACK, D. S. DUVALL and D. F. PAULONIS, *Mater. Sci. Eng.* **13** (1974) 51.
20. S. FOX, J. W. BROOKS, M. H. LORETTO and R. E. SMALLMAN, in "Strength of Metals and Alloys", edited by H. J. McQueen, J.-P. Bailon, J. I. Dickson, J. J. Jonas, and M. G. Akben, Vol. I (Pergamon. Oxford, 1985) p. 399.

Received 5 March
and accepted 15 May 1987